ELSEVIER

Thermochimica Acta 388 (2002) 143–150

thermochimica acta

www.elsevier.com/locate/tca

A mechanistic study of a topochemical dihydrogen to covalent bonding transformation

Radu Custelcean[1], James E. Jackson[*]

Department of Chemistry, Michigan State University, East Lansing, MI 48824-1322, USA

Received 23 July 2001; received in revised form 15 October 2001; accepted 18 October 2001

Abstract

Solid-state decomposition of the dihydrogen-bonded complex $LiBH_4$·TEA (TEA: triethanolamine) into a covalent material was probed via ^{11}B MAS NMR and FT-IR spectroscopies, as well as single-crystal and powder X-ray diffraction and optical microscopy. Based on variable-temperature kinetic analysis and H/D exchange experiments, H_2 loss appears to occur via rate-limiting proton transfer from the TEA's –OH groups to the BH_4^- anions at the reactant/product interface. The activation parameters $\Delta H^{\ddagger} = 84 \pm 10$ kJ/mol and $\Delta S^{\ddagger} = -70 \pm 26$ J/(mol K) are comparable to those found for neutral aqueous hydrolysis of BH_4^-, suggesting similar mechanisms for the solid and solution decompositions.

Keywords: Borohydrides; Dihydrogen bonding; Solid-state kinetics; Solid-state NMR; Topochemical reactions

1. Introduction

Organic solid-state reactions have been reported to occur since the beginning of organic chemistry. Wöhler's famous transformation in 1828 of ammonium cyanate into urea was proven to take place both in solution and solid state [1]. However, it was not until relatively recently that this discipline has developed into a mature field, with the invaluable assistance of physical methods like X-ray crystallography, optical and electronic microscopies, thermal analysis, and solid-state NMR spectroscopy. A fundamental difference between the reactivity in fluid and solid phases is that while the former is dominated by the electronic properties of molecules, reactivity in solids is a balance between packing and electronic effects. In the solid state, the reactants are usually locked in a fixed orientation with relatively low mobility, and consequently the intrinsic reactivity of the molecules is often less important than their spatial arrangement relative to the neighboring molecules in the crystal. Reactions under such geometrical control can therefore be highly selective, leading sometimes to products and materials otherwise inaccessible [2]. The first to recognize this powerful concept was G.M.J. Schmidt, who in the 1960s articulated the ''topochemical'' principle of lattice control over the course of solid-state reactions and stereochemistry of the products [3]. This approach has ever since been extensively exploited for the assembly of both small molecules and extended covalent networks with controlled

[*] Corresponding author. Fax: +1-517-353-1793.
E-mail addresses: custelce@cems.umn.edu (R. Custelcean), jackson@cem.msu.edu (J.E. Jackson).
[1] Present address: Department of Chemical Engineering and Materials Science, University of Minnesota, 421 Washington Ave SE, Minneapolis, MN 55455. Fax: +1-612-626-7246.

0040-6031/02/$ – see front matter
PII: S0040-6031(02)00023-0

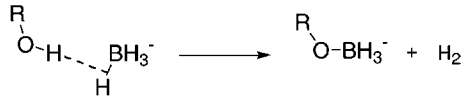

Scheme 1.

topologies [4]. However, its major disadvantage is the lack of solid-state reactivity in many systems due to misalignment of the reactive functionalities in their crystals. This obstacle can, in favorable cases, be surmounted by carefully designing the structures and solid-state reactivities of the initial molecular solids [5]. However, with the crystal engineering field still in its infancy, the development of solid-state reactive organic systems of even relatively low complexity remains challenging and time-consuming.

We have recently developed a general strategy for the topochemical assembly of covalent materials by conveniently exploiting the unconventional O–H···H–B hydrogen bonds (dihydrogen bonds) [6] between –OH groups and BH_4^- anions, representing the protonic and hydridic partners, respectively [7]. The intrinsic ability of these dihydrogen-bonded systems to lose H_2 in the solid state, and trade the weak H···H interactions for strong O–B covalent bonds (Scheme 1), makes this strategy a practical approach toward solid-state synthesis of new covalent materials with desired architectures and functions.

Our initial efforts toward the topochemical assembly of covalent materials using dihydrogen bonds have concentrated on the investigation of solid-state structures and reactivities of triethanolamine (TEA) complexes with various metal borohydrides (MBH_3X·TEA; M = Na, Li; X = H, CN) [7b–d]. A few key factors such as the relative acidity and basicity of the protonic and hydridic partners and the melting points of these dihydrogen-bonded complexes were recognized to be critical for the solid-state chemistry of these systems. Thus, within this series, the $LiBH_4$·TEA (**1**) complex proved to be particularly reactive, presumably because of the strong complexation by the Li^+ cation, which, in turn, was translated into enhanced acidity of the OH groups, and consequently extremely short H···H contacts [7d]. This fact, in conjunction with the high melting point of **1**, allowed us to address the detailed mechanism of these dihydrogen to covalent bonding transformations both at the macroscopic and the molecular levels [7b].

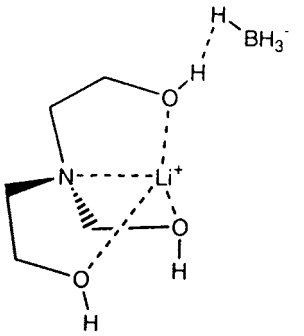

1

2. Experimental

FT-IR spectra were measured in KBr pellets on a Perkin-Elmer Spectrum 2000 instrument. ^{11}B (128.33 MHz) solid-state MAS NMR spectra were recorded on a Varian VXR-400 instrument, using solid boric acid as reference. X-ray powder diffraction measurements were conducted on a Rigaku-Denki RW400F2 diffractometer with monochromatic Cu Kα radiation, operated at 45 kV and 100 mA. Optical micrographs were obtained with a Nikon AFX-DX microscope equipped with a Mettler FP82HT hot stage. Analysis of the hydridic content was done by titration with dilute HCl and volumetric measurement of the H_2 evolved.

2.1. *In situ* ^{11}B *MAS solid-state NMR*

All spectra were recorded at a MAS frequency of 3.8 kHz, using 2.0 μs π/2 pulses, with a recycle delay of 5 s, to allow full relaxation of all boron species [8]. For each experiment, 48 scans were acquired. The observed spectra were deconvoluted into Lorentzian lines, and the ratios of the resulting integrals, corresponding to product and starting material, respectively, were used to estimate the extent of decomposition.

2.2. *H/D isotope exchange experiments*

Aliquots of 0.1–0.3 g of $LiBH_4$·TEA-d_3 were heated under dry Ar at 85–110 °C, monitoring the decompositions by H^- analysis. The partly or fully decomposed samples were analyzed by IR (KBr) and ^1H NMR (CH_3CN-d_3). No signals for the ν_{BD} in the IR

or for OH in ^{1}H NMR spectra were observed throughout the reaction.

3. Results and discussion

The crystal structure of **1** consists of $\{Li^+(TEA)\}_2$ dimers interconnected by dihydrogen bonds between the OH groups from TEA and hydridic hydrogens from BH_4^- anions, forming a one-dimensional extended network (Fig. 1). Solid-state decomposition of **1** at 120 °C under an Ar atmosphere for 1 h resulted in an insoluble refractory material. Based on the crystal structure of **1**, the finding that three moles of H_2 were lost per mole of initial complex (based on chemical analysis and TGA), and the solid-state ^{11}B MAS NMR spectrum, which showed a single peak at $\delta = -4.6$ ppm (relative to $B(OH)_3$), we proposed a one-dimensional polymeric trialkoxyborohydride structure for the final decomposed covalent product (**2**).

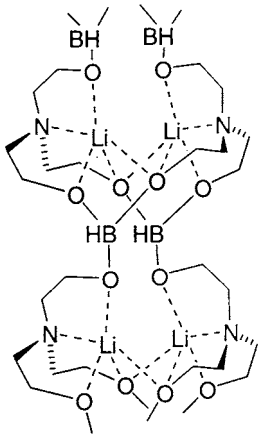

2

The formation of **2** appears to be topochemical, since a polymeric borate and unconverted $LiBH_4$ resulted from decomposition in DMSO solution. This outcome is not unexpected, as the intermediate $BH_x(OR)_{4-x}^-$ species are usually more reactive than BH_4^-, and prone to disproportionation. For comparison, no such disproportionation occurs during the solid-state decomposition, as demonstrated by H/D isotopic labeling experiments [7b]. The X-ray powder pattern

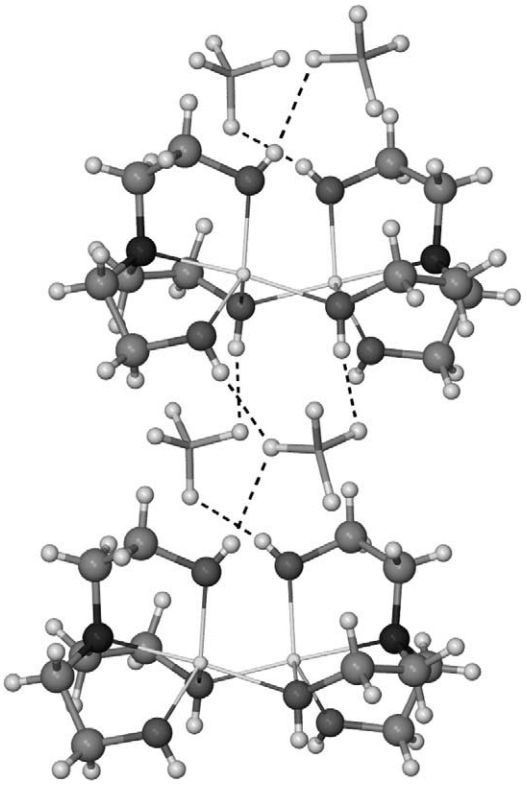

Fig. 1. X-ray crystal structure of **1**.

of **2** exhibits two broad peaks, indicating some degree of long-range organization. However, further annealing at 120 °C induced complete loss of order, pointing out the metastable nature of this topochemically generated material.

Fig. 2 presents typical optical micrographs showing crystals of **1** at different stages of decomposition at 110 °C. The initial transparent crystals gradually became opaque as the reaction progressed toward completion, suggesting the separation of a new phase. There is no visible reaction front advancing through the crystal; instead, the process appears to start randomly and proceed uniformly in the crystal bulk. The size and morphology of the crystals remained virtually unchanged during decomposition, practically eliminating the possibility of melting. However, when decomposition was examined with polarized light, a gradual disappearance of crystallinity could be observed.

As thermally initiated solid-state reactions that yield both solid and gaseous products, decompositions of **1** and other dihydrogen-bonded systems are

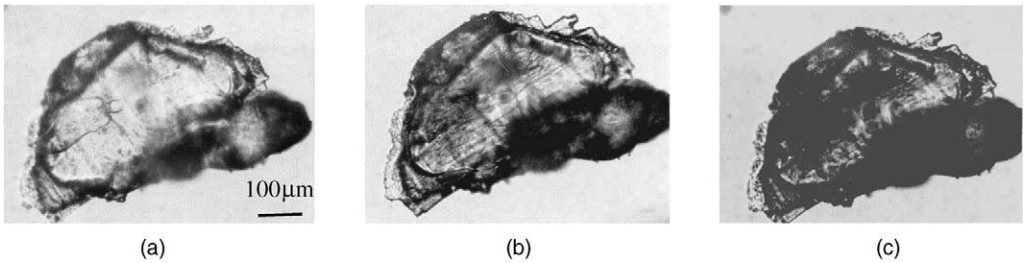

Fig. 2. Optical microscopic view (transmitted light) of $LiBH_4$·TEA solid-state decomposition: (a) initial crystal; (b) 10 min at 110 °C; (c) final decomposed crystal.

complex processes involving not only chemical steps such as breaking and formation of bonds, but also physical transformations like destruction of the initial lattice, reactant/product solid solution formation (with possible separation of the product phase), diffusion and desorption of H_2, and heat transfer. We were particularly interested in the mechanism of the solid-state **1** → **2** transformation at the molecular level, which besides its relevance to the future design of topochemically controlled reactions, is also important for a better understanding of such fundamental processes as proton transfer or covalent bond formation, extensively studied in the gas phase or solution, but considerably less in the solid state. Since conventional solid-state kinetic analyses (based on monitoring the mass loss, heat exchanged, or evolution of volume or pressure) typically yield overall kinetic parameters, which in most cases cannot be associated with particular steps of the global process [9], we opted for a more chemically specific technique for our mechanistic study. Thus, in situ ^{11}B solid-state MAS NMR spectroscopy proved to be particularly convenient for monitoring our system. Only the initial BH_4^- and the final trialkoxyborohydride could be detected throughout the reaction, presumably because of the short lifetime of the intermediate mono- and dialkoxyborohydride species. Integration of the two well-separated peaks allowed for direct measurement of the reaction extent, independent of other physical transformations that accompanied the chemical process.

We studied the solid-state decomposition of **1** at temperatures between 105 and 120 °C, using $LiBH_4$·TEA samples from the same batch for each experiment to eliminate any possible error introduced by sample variation. The resulting conversion–time

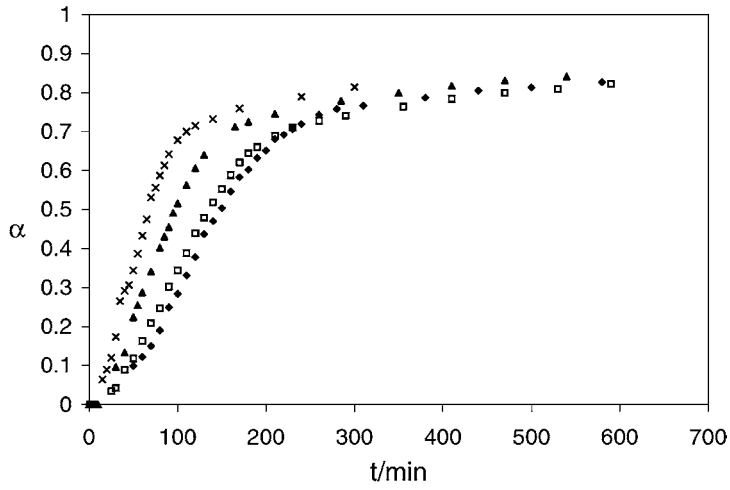

Fig. 3. Conversion (α) vs. time curves for the solid-state decomposition of **1**: (◆) 105 °C; (□) 110 °C; (▲) 115 °C; (×) 120 °C.

curves (Fig. 3) have the typical sigmoid shape characteristic for most solid-state decompositions of the type $A_{solid} \rightarrow B_{solid} + C_{gas}$ [10]. The short induction period is followed by a rapid increase in reaction rate up to the inflection point, after which time, the rate decreases monotonically to zero. This pattern is almost universally associated with the initiation of reaction at specific sites followed by the growth of nuclei, with the reaction mostly confined to the product/reactant interface. The kinetics is therefore controlled by the number of nuclei present and the total area of the expanding interface. After the inflection point, the growing nuclei start to coalesce, slowing the decomposition rate as the interfacial area decreases, until the reaction eventually stops.

Different kinetic models with their corresponding equations $g(\alpha) = kt$ (where α = fractional conversion) have been elaborated to account for various solid-state decomposition mechanisms [9,10]. Among them, the most common are the Avrami–Erofeev Eq. (1) and the phase boundary model (2):

$$[-\ln(1-\alpha)]^{1/n} = kt, \quad n = 1{-}4 \tag{1}$$

$$1-(1-\alpha)^{1/n} = kt, \quad n = 1{-}3 \tag{2}$$

The first one corresponds to a nucleation and growth mechanism, while the second is associated with an inward advancement of the reaction interface from the crystal's edges. It should be pointed out, however, that very often there is no single model that can acceptably describe the whole conversion range, as different mechanisms may operate for different stages of decomposition. The agreement of our data to Eqs. (1) and (2) as well as to other models for solid-state decompositions [9,10] were compared, and the best match was found for a nucleation and two-dimensional growth mechanism. The corresponding plots of $[-\ln(1-\alpha)]^{1/2}$ against time for different temperatures studied are presented (Fig. 4), together with the obtained rate constants k, the correlation coefficients of the linear regression analysis R^2, and the conversion ranges for which the Avrami–Erofeev law is obeyed (Table 1). It could be speculated that the two-dimensional expansion of nuclei might originate in the crystal structure of **1**, consisting of one-dimensional dihydrogen-bonded ribbons linked by conventional H-bonds in overall extended layers. Once decomposition has started, it is more likely it will propagate

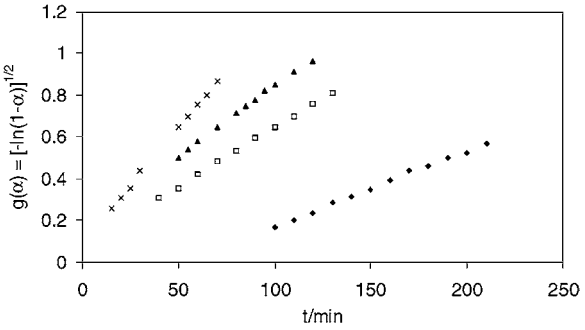

Fig. 4. Plots of the Avrami–Erofeev law, $[-\ln(1-\alpha)]^{1/2}$ against time, for the solid-state decomposition of **1**: (◆) 105 °C; (□) 110 °C; (▲) 115 °C; (×) 120 °C.

within the same layer, where the H-bonding network is disrupted, weakening thus the compactness of the crystalline environment. By comparison, a similar mechanism, but with a three-dimensional growth of nuclei ($n = 3$), gave a worse match (average $R^2 = 0.9852$ versus 0.9984 for $n = 2$). However, a totally unambiguous choice of the reaction model is practically impossible based solely on the existing kinetic data [11], and additional high resolution microscopy studies would be necessary to validate the assigned mechanism. For the late stages of decomposition, although the two- or three-dimensional contracting mechanisms (Eq. (2)) fit somewhat better than other decomposition models, they do not provide an acceptable description of our data. The measured rate constants for the solid-state decomposition of **1** at temperatures between 105 and 120 °C obey the Arrhenius equation ($R^2 = 0.9755$), as illustrated by the linear dependence of $\log k$ against $1/T$ (Fig. 5). For comparison, when the rate constants were derived from a three-dimensional growth model, a much

Table 1
Rate constants (k) for the solid-state decomposition of **1**, calculated from the Avrami–Erofeev law for nucleation and two-dimensional growth in the specified conversion ranges, together with the correlation coefficients of the linear regression analysis (R^2)

Temperature (°C)	k ($\times 10^4$ min^{-1})	Conversion range	R^2
105	37 ± 1.4	0.284–0.681	0.9980
110	56 ± 2.6	0.090–0.480	0.9988
115	66 ± 2.8	0.224–0.606	0.9979
120	111 ± 0.9	0.064–0.531	0.9990

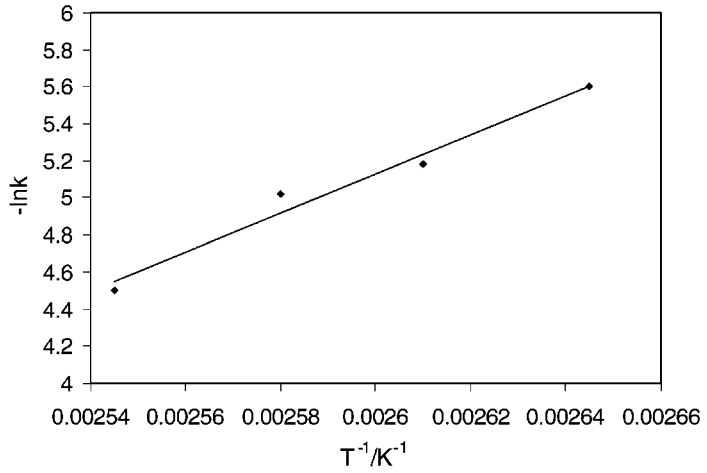

Fig. 5. Arrhenius plot for the solid-state decomposition of **1** at 105–120 °C.

worse linearity of the Arrhenius equation was obtained ($R^2 = 0.9262$), which substantiates once again the proposed two-dimensional growth mechanism. An activation energy of 88 ± 10 kJ/mol for the solid-state decomposition of **1** can be estimated from our data. Similarly, using the Eyring equation, the activation parameters for decomposition, $\Delta H^{\neq}$ and $\Delta S^{\neq}$, were calculated to be 84 ± 10 kJ/mol and −70 ± 26 J/(mol K), respectively.

An alternative approach for the kinetic analysis of solid-state reactions, which avoids the ambiguity and subjectivity associated with the model-fitting methods, is the isoconversional method, applied under isothermal or nonisothermal conditions [9,11,12]. This strategy allows the estimation of the activation energy without assuming a particular reaction model, and is particularly convenient for analysis of nonisothermal data such as that obtained from DSC and TGA experiments. Under the isothermal regime, the activation energy at a particular conversion, E_α, can be evaluated using Eq. (3) [11,12]:

$$-\ln t_{\alpha,i} = \ln\left[\frac{A}{g(\alpha)}\right] - \frac{E_\alpha}{RT_i} \quad (3)$$

While in some cases it can unmask the complexity of the solid-state process studied, one inconvenience of this method is that the obtained activation energy typically varies significantly with the extent of reaction, which complicates the interpretation of the kinetic data. We applied Eq. (3) to our data, and the resulting E_α versus α plot is illustrated in Fig. 6. The activation energies thus obtained are, within

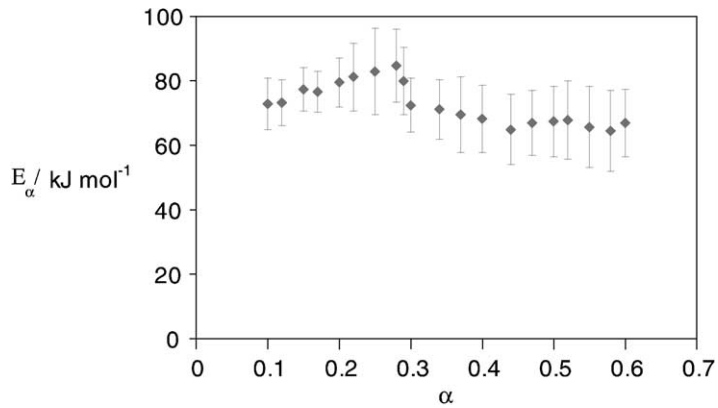

Fig. 6. Variation of activation energy with conversion for the solid-state decomposition of **1**, obtained by isoconversional method.

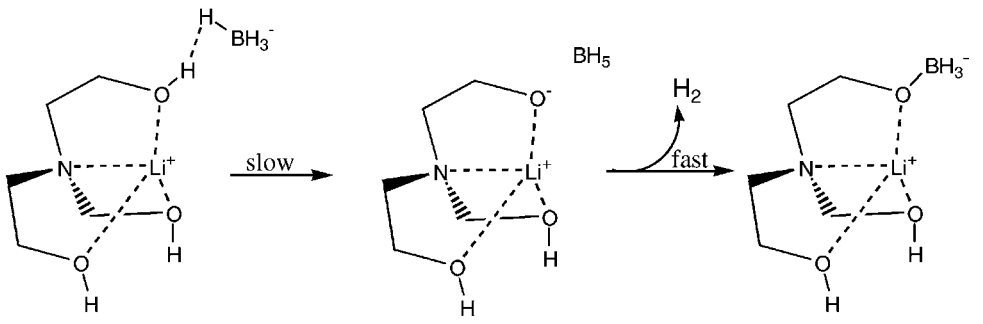

1

Fig. 7. Proposed mechanism for the first B–H···H–O to B–O transformation in **1**.

experimental errors, generally comparable with the value calculated using the model-fitting method.

Since the kinetic measurements were done by in situ ^{11}B NMR spectroscopy which allowed direct monitoring of the appearance of the final trialkoxyborohydride product, independent of other physical processes such as nucleation, phase separation, or diffusion and desorption of H_2, and considering the fact that no phase transition occurred prior to decomposition, as shown by powder X-ray diffraction, it is reasonable to assume that the kinetic parameters found in this study are directly related to the chemical transformations responsible for decomposition. Moreover, the present activation parameters are comparable with the activation enthalpy of 86 ± 4 kJ/mol and activation entropy of -93 ± 13 J/(mol K) found for the hydrolysis of BH_4^- in neutral water, and associated with the rate limiting proton transfer step [13]. However, the mechanism could be different in the solid state, with the H_2 evolution slowed down by the crystal constraints, possibly becoming the rate-determining step. To address this question, we studied the solid-state decomposition of $LiBH_4{\cdot}N(CH_2CH_2OD)_3$, the analogue of **1**, with the OH groups deuterated. H/D exchange between BH_4^- and OD groups of the TEA is expected for a scheme involving fast, reversible proton transfer followed by slow H_2 loss. However, no H/D exchange was observed at any stage of decomposition, under various conditions, as indicated by the IR or ^{1}H NMR of the partly or fully decomposed deuterated complex. This experiment suggests that as in solution, the proton transfer is slow compared to H_2 loss and B–O covalent bond formation (Fig. 7). The measured activation parameters for the solid-state decomposition of **1** can therefore be associated with the proton transfer at the reaction interface. The reacting partners in this region are presumably more flexible than in the perfectly ordered environment of the undisturbed crystal. The lower activation entropy found for this process, compared to the similar reaction in water, could be attributed to the pre-organization imposed by the dihydrogen bonding network in the crystal. Despite the heterogeneous nature of decomposition, the topochemical information is nonetheless transferred through the interface, to the newly formed covalent product.

In summary, we have reported the first in-depth mechanistic study of a topochemical dihydrogen to covalent bonding conversion. In situ ^{11}B MAS solid-state NMR spectroscopy proved to be a very convenient, chemically-specific technique, for measuring the kinetics of this decomposition, providing insight into the actual chemical transformations at the molecular level, independent of other physical processes that typically obscure the interpretation of kinetic parameters. This technique may be generally suitable for the study of other solid-state conversions, where detailed information about the involved molecular transformations are desired [14].

References

[1] (a) J.v. Leibig, F. Wöhler, Ann. Phys. Leipzig, Ser. 2 20 (1830) 369;
(b) J.D. Dunitz, K.D.M. Harris, R.L. Johnston, B.M. Kariuki, E.J. MacLean, K. Psallidas, W.B. Schweizer, R.R. Tykwinski, J. Am. Chem. Soc. 120 (1998) 13274.
[2] (a) Y. Ohashi, Reactivity in Molecular Crystals, Kodansha, Tokyo, 1993;

(b) N.B. Singh, R.J. Singh, N.P. Singh, Tetrahedron 50 (1994) 6441.
[3] G.M.J. Schmidt, Pure Appl. Chem. 27 (1971) 647.
[4] (a) J.H. Kim, S.V. Lindeman, J.K. Kochi, J. Am. Chem. Soc. 123 (2001) 4951;
(b) V. Buchholz, V. Enkelmann, Mol. Cryst. Liq. Cryst. 356 (2001) 315;
(c) J.D. Ranford, J.J. Vittal, D.Q. Wu, Angew. Chem. Int. Ed. 37 (1998) 1114;
(d) O. Herzberg, M. Epple, Eur. J. Inorg. Chem. (2001) 1395;
(e) G. Wegner, Pure Appl. Chem. 49 (1977) 443;
(f) M. Hasegawa, Chem. Rev. 83 (1983) 508;
(g) L. Addadi, M. Lahav, J. Am. Chem. Soc. 101 (1979) 2152;
(h) J.L. Foley, L. Li, D.J. Sandman, M.J. Vela, B.M. Foxman, R. Albro, C.J. Eckhardt, J. Am. Chem. Soc. 121 (1999) 7262.
[5] (a) L. Leiserowitz, G.M.J. Schmidt, J. Chem. Soc. A (1969) 2372;
(b) K.S. Feldman, R.F. Campbell, J. Org. Chem. 60 (1995) 1924;
(c) A. Matsumoto, T. Odani, M. Chikada, K. Sada, M. Miyata, J. Am. Chem. Soc. 121 (1999) 11112;
(d) J. Xiao, M. Yang, J.W. Lauher, F.W. Fowler, Angew. Chem. Int. Ed. 39 (2000) 2132;
(e) G.W. Coates, A.R. Dunn, L.M. Henling, J.W. Ziller, E.B. Lobkovsky, R.H. Grubbs, J. Am. Chem. Soc. 120 (1998) 3641;
(f) L.R. MacGillivray, J.L. Reid, J.A. Ripmeester, J. Am. Chem. Soc. 122 (2000) 7817.
[6] R. Custelcean, J.E. Jackson, Chem. Rev. 101 (2001) 1963.
[7] (a) R. Custelcean, M. Vlassa, J.E. Jackson, Angew. Chem. Int. Ed. 39 (2000) 3299;
(b) R. Custelcean, J.E. Jackson, J. Am. Chem. Soc. 122 (2000) 5251;
(c) R. Custelcean, J.E. Jackson, J. Am. Chem. Soc. 120 (1998) 12935;
(d) R. Custelcean, J.E. Jackson, Angew. Chem. Int. Ed. 38 (1999) 1661.
[8] H. Eckert, Prog. Nucl. Magn. Reson. Sp. 24 (1992) 159.
[9] (a) S. Vyazovkin, C.A. Wight, Annu. Rev. Phys. Chem. 48 (1997) 125;
(b) S. Vyazovkin, Int. Rev. Phys. Chem. 19 (1) (2000) 45.
[10] (a) N.B. Hannay, Reactivity of Solids Treatise on Solid-state Chemistry, Vol. 4, Reactivity of Solids, Plenum Press, New York, 1976;
(b) M.E. Brown, D. Dollimore, A.K. Galwey, in: C.H. Bamford (Ed.), Comprehensive Chemical Kinetics, Vol. 22, Reactions in the Solid State, Elsevier, Amsterdam, 1980.
[11] S. Vyazovkin, C.A. Wight, Thermochim. Acta 340–341 (1999) 53.
[12] S. Vyazovkin, C.A. Wight, J. Phys. Chem. A 101 (1997) 8279.
[13] R.E. Mesmer, W.L. Jolly, Inorg. Chem. 1 (1962) 608.
[14] A.K. Galwey, M.E. Brown, J. Therm. Anal. Calorim. 60 (3) (2000) 863.